

LA-UR- 01-0390

Approved for public release;  
distribution is unlimited.

C. I

36

*Title:* Functionally Graded MoSi<sub>2</sub>-Al<sub>2</sub>O<sub>3</sub> Tubes for Temperature Sensor Application

*Author(s):* M. I. Peters  
R. U. Vaidya  
R. G. Castro  
J. J. Petrovic  
K. J. Hollis  
D. E. Gallegos

*Submitted to:* Functionally Graded Materials Conference/ACERS Metting  
(2000)  
Estes Park, Colorado  
September 11-14, 2000



**Los Alamos**  
NATIONAL LABORATORY

Los Alamos National Laboratory, an affirmative action/equal opportunity employer, is operated by the University of California for the U.S. Department of Energy under contract W-7405-ENG-36. By acceptance of this article, the publisher recognizes that the U.S. Government retains a nonexclusive, royalty-free license to publish or reproduce the published form of this contribution, or to allow others to do so, for U.S. Government purposes. Los Alamos National Laboratory requests that the publisher identify this article as work performed under the auspices of the U.S. Department of Energy. Los Alamos National Laboratory strongly supports academic freedom and a researcher's right to publish; as an institution, however, the Laboratory does not endorse the viewpoint of publication or guarantee its technical correctness.

## FUNCTIONALLY GRADED $\text{MoSi}_2\text{-Al}_2\text{O}_3$ TUBES FOR TEMPERATURE SENSOR APPLICATIONS

M.I. Peters, R. U. Vaidya, R. G. Castro, J.J. Petrovic, K.J. Hollis and D.E. Gallegos

Los Alamos National Laboratory  
Material Science and Technology Division  
Los Alamos, NM 87545, USA

### ABSTRACT

$\text{MoSi}_2$  and  $\text{Al}_2\text{O}_3$  are thermodynamically stable elevated temperature materials whose thermal expansion coefficients match closely. Composites of these materials have potential for applications such as protective sheaths for high temperature sensors.  $\text{MoSi}_2\text{-Al}_2\text{O}_3$  functionally graded tubes were fabricated using advanced plasma spray-forming techniques. Both continuously-graded and layered-graded tube microstructures were synthesized. The characteristics of the graded microstructures and the features of the graded mechanical properties of these tubes will be discussed.

### INTRODUCTION

Using platinum coatings on alumina ( $\text{Al}_2\text{O}_3$ ) sheaths for thermocouples is a widely used practice in the glass industry. Protection of the thermocouple wires and alumina ( $\text{Al}_2\text{O}_3$ ) sheathing is necessary to avoid corrosion and dissolution of the temperature-sensing unit. The cost associated with providing platinum coatings on the  $\text{Al}_2\text{O}_3$  sheath material can be prohibitively high when taking into consideration the infrastructure needed at the glass plants to maintain and secure an inventory of available platinum. There are also issues associated with improving the performance of the platinum coated  $\text{Al}_2\text{O}_3$ . The failure rate of the thermocouples can be as high as 50%. The U.S. glass industry has been in search of alternative materials that can replace platinum and still provide the durability and performance needed to survive in an extremely corrosive glass environment.

Investigations by Y.S. Park et al [1] have shown that molybdenum disilicide ( $\text{MoSi}_2$ ) has similar performance properties in molten glass as some refractory materials that are currently being used in glass processing applications. Molybdenum disilicide is a candidate high temperature material for such applications because of its high melting temperature (2030°C), relative low density (6.24g/cm<sup>3</sup>), high thermal conductivity (52 W/mK), a brittle to ductile transition near 1000°C, and stability in a variety of corrosive and oxidative environments [2,3]. Additionally, the cost of  $\text{MoSi}_2$  is significantly lower as compared to platinum coatings.

Plasma spraying has been shown to be a very effective method for producing coatings and spray formed components of  $\text{MoSi}_2$  and  $\text{MoSi}_2$  composites [4]. Investigations on plasma spray formed  $\text{MoSi}_2\text{-Al}_2\text{O}_3$  composite gas injection tubes were shown to have enhanced high temperature thermal shock resistance when immersed in molten copper and aluminum [5]. The composite tubes outperformed high-grade graphite and SiC tubes when immersed in molten copper and had similar performance to high-density graphite and mullite when immersed in molten aluminum. Energy absorbing mechanisms such as debonding (between the  $\text{MoSi}_2$  and  $\text{Al}_2\text{O}_3$  layers) and microcracking in the  $\text{Al}_2\text{O}_3$  layer contributed to the composites' ability to absorb

thermal stresses and strain energy during the performance test (shown in Figure 1). Molybdenum disilicide and alumina are chemically compatible and have similar thermal expansion coefficients [6,7].

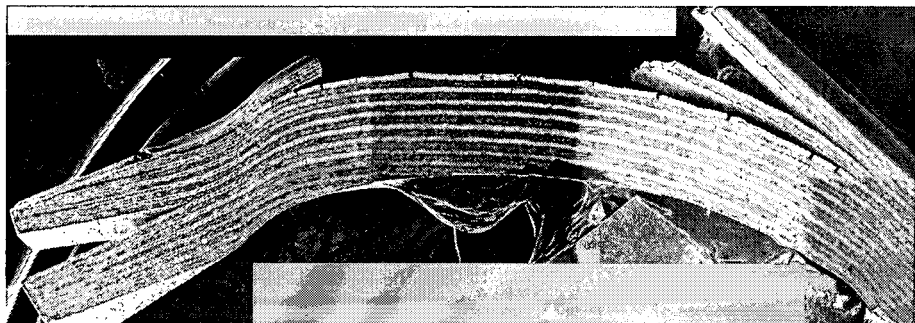


Figure 1. Four-point bend test beam after testing at 1400°C. Extensive debonding at the MoSi<sub>2</sub>/Al<sub>2</sub>O<sub>3</sub> interface and cracking within the Al<sub>2</sub>O<sub>3</sub> was observed [5].

For thermocouple applications that require immersion of the thermocouple directly into molten glass, MoSi<sub>2</sub> coatings on Al<sub>2</sub>O<sub>3</sub> protective sheaths will need to be optimized in order to perform in both a high-temperature (>1300°C) oxidizing environment (above the glass line) in addition to performing in the highly corrosive molten glass environment (below the glass line). We are currently evaluating the potential use of a graded coating of Al<sub>2</sub>O<sub>3</sub> to MoSi<sub>2</sub> to enhance the performance of the MoSi<sub>2</sub> coating in molten glass. The graded microstructure of the coating will reduce the residual stresses that can develop during the spray deposition process, which can cause cracking and spallation of the coating limiting the coatings' lifetime. Preliminary results will be presented on the methodology used to produce the plasma sprayed MoSi<sub>2</sub>-Al<sub>2</sub>O<sub>3</sub> graded composites and on the microstructure and mechanical behavior.

#### EXPERIMENTAL PROCEDURES

Use of conventional plasma spraying equipment allows the flexibility of producing a variety of MoSi<sub>2</sub>-Al<sub>2</sub>O<sub>3</sub> microstructures, including laminate and graded structures. The plasma spraying equipment used for producing the graded structures included a Praxair Surface Technologies SG100 plasma torch and two Model 1264 powder feed hoppers. The plasma torch was mounted on a Fanuc S10 6-axis robot. A Technar DPV 2000 in-flight particle analyzer was used to measure the temperature, velocity and particle distribution of the MoSi<sub>2</sub> and Al<sub>2</sub>O<sub>3</sub> particles as they exited the plasma torch. A computer control system was used to monitor and control the processing gases and the powder hoppers dispensing rate. Figure 2 shows an example of the computer control logic that was used to control the powder hopper rotation speed needed to produce the MoSi<sub>2</sub>- Al<sub>2</sub>O<sub>3</sub> graded structure. In this figure, pure Al<sub>2</sub>O<sub>3</sub> (Powder 2) is first deposited at a powder hopper rotation speed of 0.8 rpm. After an initial period of depositing pure Al<sub>2</sub>O<sub>3</sub>, MoSi<sub>2</sub> (Powder 1) is gradually introduced into the plasma torch by increasing the powder hopper rotational speed for MoSi<sub>2</sub> and decreasing the rotational speed for Al<sub>2</sub>O<sub>3</sub>. The powder hopper speed for MoSi<sub>2</sub> subsequently reaches 0.8 rpm and the Al<sub>2</sub>O<sub>3</sub> powder dispensing speed goes to zero. Pure MoSi<sub>2</sub> is then deposited on the outside diameter of the tube. Argon was used for the plasma generating gas (40 standard liters per minute, slm) and as a carrier gas for the MoSi<sub>2</sub> and Al<sub>2</sub>O<sub>3</sub> powders (1 to 4 slm). A Mikron TH 4104 infrared camera was used to measure and display the temperature of the substrate. A POCOTM graphite tube (12.7mm OD, 9.5mm ID) was used as the substrate for the deposition spray trials.

To determine the mechanical behavior of the graded  $\text{MoSi}_2\text{-Al}_2\text{O}_3$  structures, C-rings were machined from the material deposited on the graphite rods. C-ring samples were wire electro-discharge machined (EDM) out of the sprayed tube samples. The C-rings had an OD of 25.93 mm, an ID of 12.8mm and a width of 10.76 mm. The critical  $b/(r_o-r_i)$  ratio was 1.64, within the required range of 1 to 4. The C-ring samples were tested in diametrical compression using a hydraulic Instron test frame (Type 1331 with an 8500 Plus controller and a 10kN load cell), at a crosshead speed of 0.125 mm/min (strain rate  $\sim 0.316 \times 10^{-4} \text{ s}^{-1}$ ). Machine compliance was corrected using a standard  $\text{Al}_2\text{O}_3$  sample of known stiffness. All of the samples were machined and tested in accordance with ASTM Standard C 1323-96. Twelve samples for each composite tube were tested. Four samples of monolithic plasma sprayed  $\text{MoSi}_2$  and  $\text{Al}_2\text{O}_3$  were tested and used for comparison. A Weibull statistical approach [8] was used to obtain the strength distributions in the coated and uncoated samples. While the standardized student-t test [8] employing the normal or gaussian frequency distribution is often used in statistical analysis, there is no theoretical or experimental justification for using it in problems involving fracture. Use of a normal distribution is often inappropriate in analyzing fracture problems with plasma-sprayed ceramic materials because of the presence of multiple flaw populations. The Weibull distribution is more appropriate (and conservative) in this scenario because it does not require that the flaw population be normally distributed.

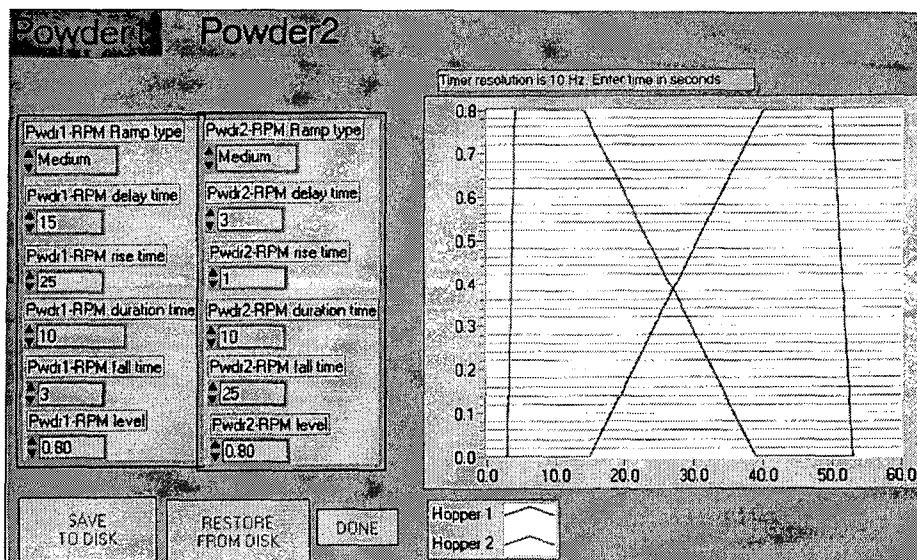


Figure 2. Computer based control system used to control the powder hopper dispensing rate for producing the  $\text{MoSi}_2\text{-Al}_2\text{O}_3$  graded structures. Powder 2 is  $\text{Al}_2\text{O}_3$  and Powder 1 is  $\text{MoSi}_2$ .

## RESULTS

Macrographs of two types of  $\text{MoSi}_2\text{- Al}_2\text{O}_3$  graded composites produced by plasma spraying are shown in Figure 3. The white phase is the  $\text{Al}_2\text{O}_3$  and the dark phase is  $\text{MoSi}_2$ . Figure 3a, shows a layered and graded microstructure where the cross-section of the sample consists of discrete individual layers that have been graded from  $\text{Al}_2\text{O}_3$  to  $\text{MoSi}_2$ . Figure 3b, shows the cross-section of a continuously graded structure where pure  $\text{Al}_2\text{O}_3$  was first deposited on a graphite rod followed by increasing amounts of  $\text{MoSi}_2$  until pure  $\text{MoSi}_2$  is deposited on the outside diameter of

the tube. An example of a typical microstructure produced in the graded region between the  $\text{MoSi}_2$  and the  $\text{Al}_2\text{O}_3$  is given in Figure 4. A layered type of microstructure is produced when individual molten particles are flattened as they impact the substrate or previously deposited material.

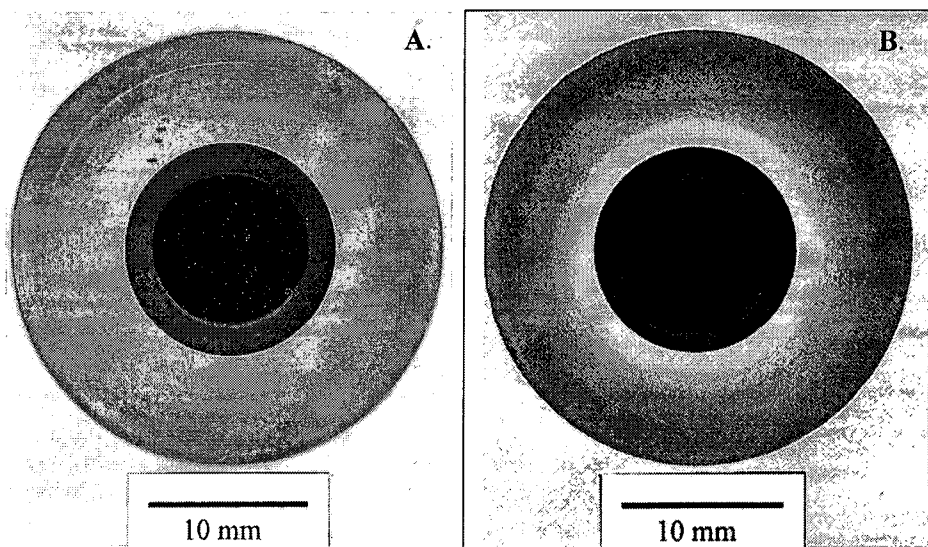


Figure 3. Macrographs of  $\text{MoSi}_2\text{-Al}_2\text{O}_3$  graded tube cross-sections. a) Discrete individual layers that have been graded from  $\text{Al}_2\text{O}_3$  to  $\text{MoSi}_2$  and b) continuously graded structure from pure  $\text{Al}_2\text{O}_3$  on the inside diameter of the tube to pure  $\text{MoSi}_2$  on the outside diameter of the tube.

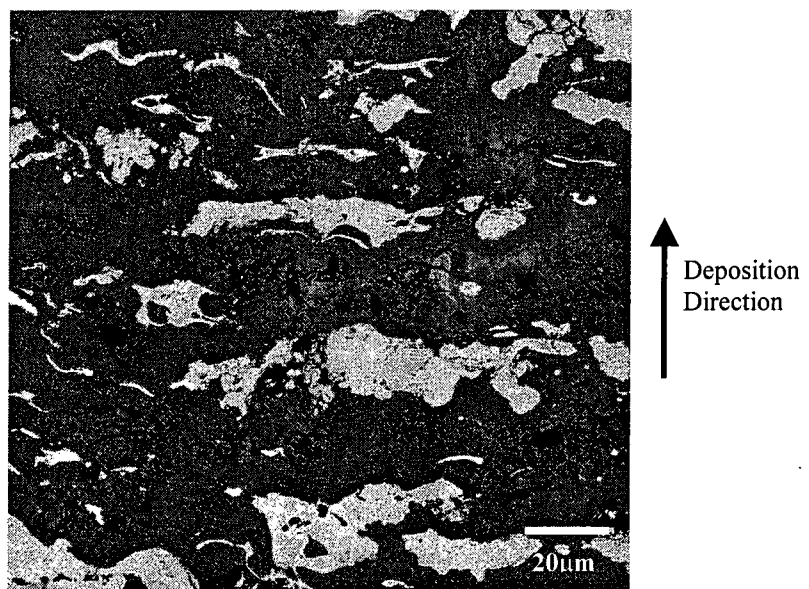


Figure 4. A typical microstructure produced in the graded regions between the  $\text{MoSi}_2$  and  $\text{Al}_2\text{O}_3$ . Light areas are  $\text{Al}_2\text{O}_3$  and dark areas are  $\text{MoSi}_2$ .

Residual stresses can occur in plasma sprayed deposited material as a result of quenching stresses that occur when individual particles are rapidly cooled upon impacting the substrate surface, differential thermal contraction between the deposited material and substrate and volume changes associated with any solid state phase transformation [9]. Residual stresses can give rise to deformation of the coated work piece and can result in spalling and cracking of the coating. In addition, various types of coating performance indicators such as adhesion strength, resistance to thermal shock under thermal cycling and erosion resistance are strongly influenced by the nature of the residual stresses. At elevated temperatures ( $> 1000^{\circ}\text{C}$ ),  $\text{MoSi}_2$  goes through a brittle to ductile transformation [2] and can accommodate some of the residual stresses that occur during the deposition process and also during high temperature use of the material. Combining  $\text{MoSi}_2$  with  $\text{Al}_2\text{O}_3$  can enhance the high temperature performance of  $\text{Al}_2\text{O}_3$  protective thermocouple sheaths by improving the poor thermal shock behavior of  $\text{Al}_2\text{O}_3$ .

#### THERMAL AND MECHANICAL PERFORMANCE

The mechanical behavior of the FGMs was evaluated using C-ring tests. Probability of failure at a given strength was obtained using Weibull analysis. Figure 5 shows the strength distribution plots for the layered and continuous FGMs. Both the continuous and layered FGM microstructures were found to exhibit similar mean Weibull strengths ( $\sim 70$  MPa). However, the spread of the data for the continuously graded material was smaller (hence a larger Weibull slope; 13.38 for the continuously graded samples, versus 7.635 for the layered graded samples). Interestingly, the fracture energy of the FGMs (qualitatively determined from the area under the load-displacement plot of the C-ring tests) was observed to be significantly higher ( $\sim 3$  times) than that of monolithic  $\text{Al}_2\text{O}_3$  or  $\text{MoSi}_2$  (monolithic  $\text{Al}_2\text{O}_3$ -285 J/m<sup>2</sup>, monolithic  $\text{MoSi}_2$ -496 J/m<sup>2</sup>, continuously graded  $\text{MoSi}_2/\text{Al}_2\text{O}_3$  composite-766J/m<sup>2</sup>, layered and graded  $\text{MoSi}_2/\text{Al}_2\text{O}_3$  composite-955J/m<sup>2</sup>). We are in the process of conducting independent fracture toughness tests to validate these preliminary observations and to determine if the graded microstructures exhibit R-curve behavior.

Fracture surfaces for the continuously graded and layered FGMs are shown in Figure 6. The fracture surface exhibited extensive microcracking and roughening in the center portion of the C-ring. We believe that the increased toughening of the composite is a direct result of microcracking. Preliminary analysis has indicated the strength and toughness of these FGM tubes to be more than acceptable for the proposed applications.

Earlier studies conducted on  $\text{MoSi}_2$  indicated that the oxidation of the  $\text{MoSi}_2$  was acceptable below and above the glass line. However, the high corrosion rate at the glass line was unacceptable and the resulting glass-line oxidation provided a challenge in the development of thermocouple sheaths. The answers to some of these challenges lies in understanding the mechanisms involved in the glass corrosion process. Figure 7 is a schematic of a phenomenological model that describes the oxidation mechanisms occurring above, at and below the glass line for  $\text{MoSi}_2$  in a borosilicate glass [1]. Above the glass line (air environment), a  $\text{SiO}_2$  coating protects the  $\text{MoSi}_2$  from continued oxidation. The protective  $\text{SiO}_2$  layer is disrupted in the temperature range around  $500^{\circ}\text{C}$  and pesting of the  $\text{MoSi}_2$  can occur. Below the glass line, molybdenum metal, oxides, and silicides form in a silicon-depleted layer. The silicon-depleted layer consists of a mixture of phases ( $\text{Mo}_5\text{Si}_3$ ,  $\text{Mo}_3\text{Si}$  and Mo) that are stable due to low oxygen activity [1].

The high flux of molten glass at the glass line increases the oxygen activity, resulting in increased oxidation rates. The oxidation rate is further accelerated by the dissolution of the protective  $\text{SiO}_2$  layer as a result of the convective flow of glass at the glass line. Efforts are underway to produce a protective  $\text{MoSi}_2$  coating to eliminate the high corrosion rate at the glass line. We are currently pursuing composite coatings of  $\text{MoSi}_2$  and higher viscosity glasses to minimize glass line corrosion rates.

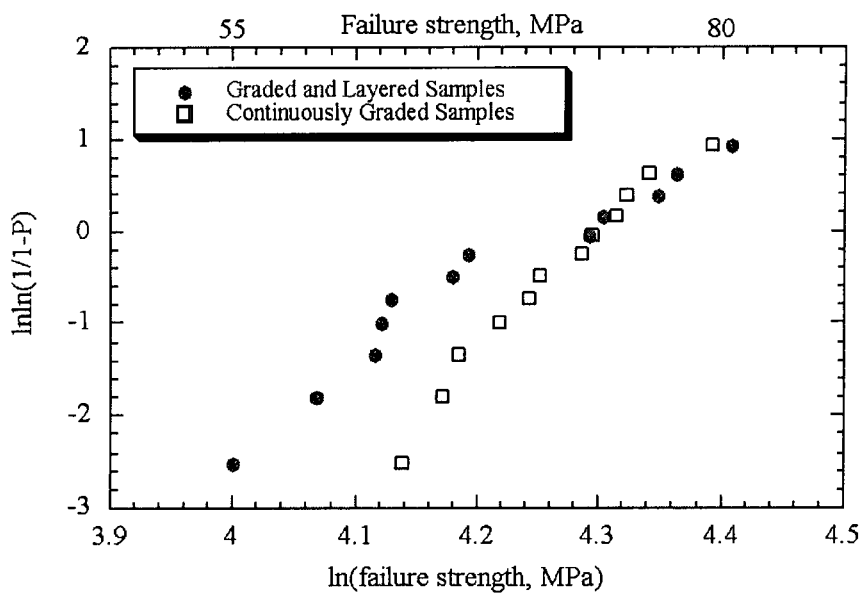


Figure 5. Results of C-ring tests performed on continuously graded and layered graded  $\text{Al}_2\text{O}_3$ - $\text{MoSi}_2$  coatings.

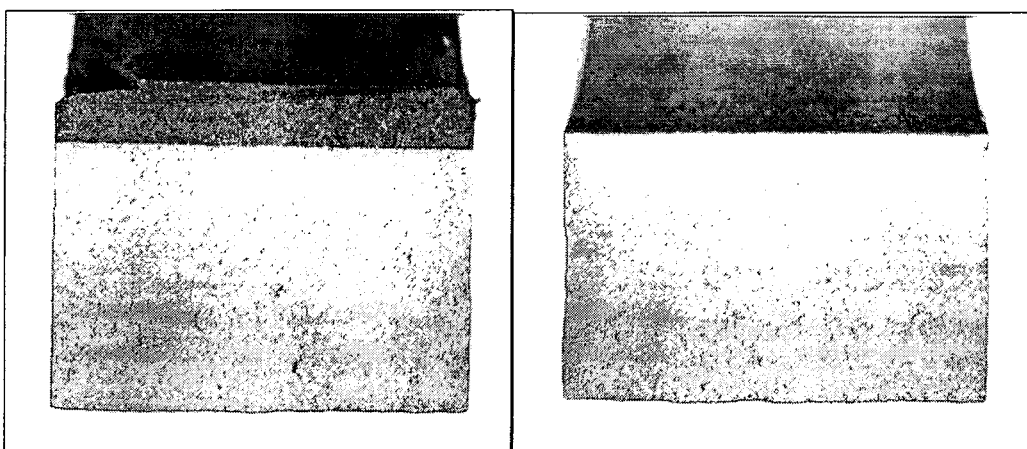


Figure 6. Macrographs of c-ring tests performed on  $\text{Al}_2\text{O}_3$ - $\text{MoSi}_2$  coatings sprayed on graphite substrates. a) Layered FGM b) Continuous FGM.

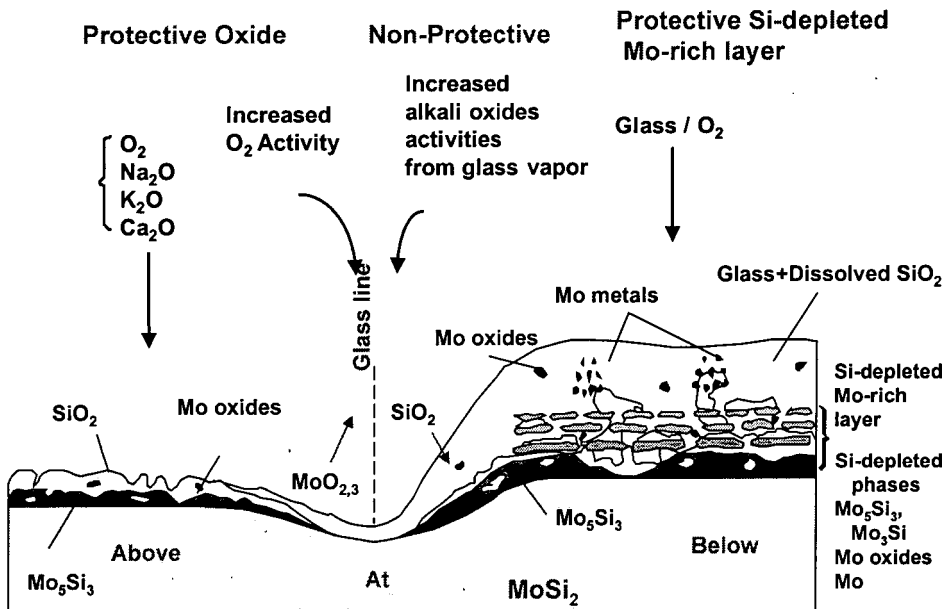


Figure 7. Schematic of model describing the oxidation of the FGM  $\text{MoSi}_2$  coating above, below and at the glass line [1].

#### CONCLUDING REMARKS

We have demonstrated the use of conventional plasma spraying equipment in manufacturing  $\text{MoSi}_2\text{-Al}_2\text{O}_3$  FGMs. The mechanical performance of these FGMs was superior to that of the monolithic materials. This was verified through C-ring tests. Although the molten glass corrosion behavior of the FGM coating is acceptable below and above the glass line, the corrosion rate at the glass line is higher than desirable. Processing of  $\text{MoSi}_2$  based FGM composite coatings is ongoing and it will be determined if these new FGM coatings will reduce the glass-line corrosion.

#### ACKNOWLEDGEMENTS

This research has been supported by the U.S. Department of Energy, Office of Industrial Technologies, Glass Industry Program. The authors would like to acknowledge the technical support given by Richard Hoover at LANL.

#### REFERENCES

- <sup>1</sup>Y.S. Park, D.P. Butt, R. Castro, J. Petrovic, W. Johnson, *Materials Science and Engineering*, **A261**, 278-283 (1999).
- <sup>2</sup>J.J. Petrovic, *Materials Research Society Bulletin*, **XVIII 35**, (1993).
- <sup>3</sup>J.J. Petrovic, and A.K. Vasudevan, *Materials Research Society Symposium Proceedings*, **322**, 3 (1994).
- <sup>4</sup>R.G. Castro, H. Kung, K.J. Hollis and A.H. Bartlett, *15<sup>th</sup> International Thermal Spray Conference*, Nice, France May 25-29, 1199-1204 (1998).
- <sup>5</sup>A.H. Bartlett, R.G. Castro, D.P. Butt, H. Kung, Z. Zurecki and J.J. Petrovic, *Industrial Heating*, January 33-36 (1996).

<sup>6</sup>R.U. Vaidya, P. Rangaswamy, M.A.M. Bourke, D.P. Butt, *Acta Metallurgica*, **46**, 2047-2061 (1998).

<sup>7</sup>W.D. Kingery, H.K. Bowen, D.R. Uhlmann, *Introduction to Ceramics*, Second Edition, John Wiley & Sons, New York, 1976.

<sup>8</sup>W. A. Weibull, *Journal of Applied Mechanics*, **18** [3], 293 (1951).

<sup>9</sup>S. Kuroda and T.W. Clyne, *Thin Solid Films*, **200**, 49-66 (1991).